Numerical Analysis of Mixed Convection Coupled with Thermal Radiation in a Ventilated Channel Containing Various Heat-Generating Blocks

Rachid Hidki, Lahcen El Moutaouakil, Mohammed Boukendil(✉), Zouhair Charqui, Zaki Zrikem, and Abdelhalim Abdelbaki

LMFE, Department of Physics, Faculty of Sciences Semlalia, Cadi Ayyad University, B.P. 2390, Marrakesh, Morocco
m.boukendil@uca.ac.ma

Abstract. In this study, thermal radiation and mixed convection in a ventilated horizontal channel are analyzed. The channel contains five cylindrical blocks that produce different volumetric heat rates. The channel is ventilated by two openings; the inlet is located on the left wall, and the outflow is on the top one. All the channel walls are adiabatic, except for the upper wall, which is held at a constant low temperature of $T_C = 20$ °C. To numerically solve the differential equations governing the current problem, a numerical code based on the finite volume approach and the SIMPLE algorithm is utilized. The discrete ordinate method is used to discretize the radiative transfer equation. The impacts of the Reynolds number and the emissivity of the surfaces on the heat transfer and fluid flow are analyzed. The numerical simulations indicate that increasing the Reynolds number or the emissivity considerably decreases the maximum temperature in the cavity and improves the performance of the considered system.

Keywords: Mixed convection · Ventilated channel · Finite volume method · Numerical simulation · Heat sources

Nomenclature

d	cylinders diameter, m
D	cylinders diameter $D = d/H$
g	gravitational acceleration, ms^{-2}
h^*	openings size $h^* = h/H$
h	openings size, m
H	cavity's height, m
i	radiation intensity, Wm^{-2}
I	dimensionless intensity
k	thermal conductivity, $Wm^{-1}K^{-1}$
K	conductivity ratio $K = k_S/k_f$
L	cavity's length, m
Nu	Nusselt number

Z. Azari et al. (Eds.): JET 2022, LNME, pp. 73–84, 2024.
https://doi.org/10.1007/978-3-031-49727-8_8

Pr	Prandtl number
Pl	Planck number
P	dimensionless pressure
Q	internal heat generation, Wm^{-3}
Ri	Richardson number
Re	Reynolds number
Ra	Rayleigh number
T_R	temperature ratio
T	dimensional temperature, °C
t	time, s
U, V	velocity components
X, Y	Cartesian coordinates

Greek symbols

σ	Stefan-Boltzmann constant, $Wm^{-2}K^{-4}$
α	thermal diffusivity, m^2s^{-1}
β	thermal expansion coefficient, K^{-1}
ε	emissivity of radiative surface
ω	scattering albedo
ϕ	phase function
θ	dimensionless temperature
υ	kinematic viscosity, m^2s^{-1}
Ω	solid angle, sr
λ	heat generation parameter
ρ	density, kgm^{-3}
τ	dimensionless time
μ, η	direction cosines
τ^*	optical thickness
ψ	dimensionless stream function

Subscripts

C	convective term, cell, or cold wall
f	fluid
i	block index
in	inlet
LR	local radiative
LC	local convective
max	maximum
R	radiative
s	solid (blocks)
T	total

Abbreviations

B	block

1 Introduction

The miniaturization of modern electronic devices has resulted in a reduction of physical space available for the components, leading to a rise in power density. Since electronic components are temperature-sensitive and can be damaged or perform poorly if their temperature falls outside the nominal operating range. Therefore, thermal dissipation has become a critical aspect of their operation. However, implementing cooling systems in compact electronic systems is often challenging, mainly when the components generate different amounts of heat or are not uniformly distributed in electronic packaging. To ensure effective cooling in these systems, it is necessary to employ convection in its three forms (forced, mixed, and natural) in conjunction with thermal radiation. Researchers are actively pursuing new cooling system designs (usually simulated using cavities containing heating bodies) that offer a balance of compactness, high performance, and cost-effectiveness [1–5].

Mixed convection (MC) occurs as a result of a combination of both free and forced convection, where the flow is impacted by both a non-uniform density distribution of the fluid and an external forcing system. Numerous numerical studies have investigated MC in cavities that contain isothermal blocks. One such study conducted by Chamkha et al. [6], analyzed two-dimensional MC surrounding an isothermal square body placed at the center of a vented air-filled cavity. The cavity's right wall is fixed at a low temperature, while the remaining walls are kept adiabatic. The study assessed the impact of various factors such as the Richardson number, Reynolds number, outlet position, position, and aspect ratio of the block on the thermal fields and flow patterns. The findings indicated that the heat transfer was optimal when the outflow was positioned at the top of the right wall. In their research, Javadzadegan et al. [7] investigated the MC heat transfer and fluid flow inside a ventilated cavity containing a hot elliptical obstacle maintained at a constant temperature. The study's main objective was to examine the impact of using a porous medium on the velocity and thermal fields.

In comparison to an isothermal block, a heat-generating block (HGB) offers a more accurate portrayal of an electrical component. A numerical investigation was carried out by Ahammad et al. [8] to examine the impact of various factors, such as the Richardson number, the solid/fluid thermal conductivity ratio, and the diameter of the HGB, on a magnetohydrodynamic MC problem in a vented cavity. The study found that a smaller block size and a lower thermal conductivity ratio improved heat transfer in the system. Ahammad et al. [9] revisited the same configuration to investigate the impact of the Reynolds, Hartmann, and Prandtl numbers on the flow and thermal fields. It was observed that these parameters have a considerable impact on both the thermal and flow fields. MC in cavities containing simple heat-conducting bodies (obstacles) has been studied in the references [10–12].

MC in channels is usually used as a methodology for designing and optimizing cooling systems for electronic equipment. Pirouz et al. [13] numerically examined the MC in a horizontal channel with upper and lower bodies mounted on the horizontal walls and receiving uniform heat flux through their base. Ghaneifar et al. [14] investigated numerically the MC of a nanofluid in an insulated horizontal channel containing two central HGBs. Hamouche and Bessaïh [15] considered a 2D channel with two identical heaters on the bottom wall. The same problem was considered by Boutina and Bessaïh [16] with an inclined channel. Hssain et al. [17] studied numerically steady MC of a nanofluid in a horizontal channel with isothermal blocks to simulate extremely heat-conductive electronic components. All these studies are agreed with the effect of ventilation (Re effect) on the behavior of the considered system.

It is important to remember that thermal radiation (TR) is necessary for cooling electronic components [18]. Numerous studies have been conducted on the coupling of natural convection (NC) and TR in closed cavities containing heating blocks of various geometrical shapes, including rectangular [19], circular [20], and square [21, 22]. These investigations reveal that TR improves total heat exchange, enabling more effective cooling of the investigated heat sources. Mandal et al. [23] and Peiravi and Alinejad [24] examine the convective heat transfer and TR in a channel with blocks. Mandal et al. [23] investigated MC with TR in a channel containing discrete heat sources on the bottom wall. Their results show that the TR interaction between the surfaces decreases with an increase in the Reynolds number. Peiravi and Alinejad [24] evaluated the combined effects of TR and MC on heat transfer between a channel's working fluid and a square solid. The results reveal that when the radiation parameter rises, the heat transfer rate decreases.

The above literature review suggests that insufficient focus has been given to TR exchange, especially when heat-generating blocks are present in channels and cavities. This study aims to demonstrate the significance of MC and TR for cooling multiple HGBs located in a horizontal channel. This research is motivated by the search for cost-effective cooling systems for high-performance computers that are both compact and powerful. The findings are displayed in terms of isotherms, streamlines, maximum temperature profiles, and those of the Nusselt number.

2 Mathematical Model and Validation

2.1 Problem Description

Figure 1 presents a schematic representation of an open cavity, highlighting its various parameters. The air-filled rectangular cavity, with dimensions of $L = 3H = 15\,\text{cm}$, contains five HGBs, representing different electronic components. The positions of the HGBs are at $X_i = 0.5i$ and $Y_i = 0.5$ with $1 \leq i \leq 5$. . The blocks having the same thermal conductivity (k_S) and diameter (d), and generate heat at varying rates, with $Q_i = \lambda_i \times Q = 1720 \times \lambda_i$, where $\lambda_i = 2^{3-i}$ is the internal heat generation parameter. All the cavity walls are kept adiabatic except the upper one, which is kept at the same temperature as the air inlet $T_C = T_{in} = 20\,°\text{C}$. The inlet and outlet are placed, respectively, on the left wall and the top wall, with equal sizes $h = h^* \times H$. The fluid enters the cavity with a velocity of u_{in}. Simulations were also carried out for $h^* = 0$, which represents a closed cavity, to show that combining TR and MC instead of NC may significantly enhance the total heat transfer.

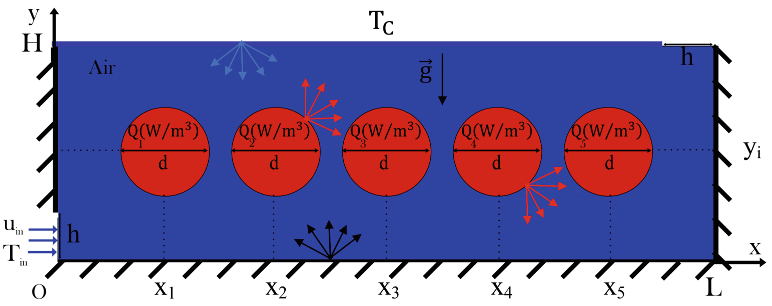

Fig. 1. Schematic configuration

2.2 Mathematical Model

The flow under examination is assumed to be two-dimensional, laminar, Newtonian, and incompressible. Except for the density in the buoyancy component, which is addressed using the Boussinesq approximation, the thermophysical characteristics of the air are maintained constant. These assumptions permit the formulation of governing equations, which are expressed in dimensionless form, including the conservation of mass, momentum, energy, and the radiative transfer equation (RTE).

$$\frac{\partial U}{\partial X} + \frac{\partial V}{\partial Y} = 0 \tag{1}$$

$$\frac{\partial U}{\partial \tau} + U\frac{\partial U}{\partial X} + V\frac{\partial U}{\partial Y} = -\frac{\partial P}{\partial X} + Pr\left(\frac{\partial^2 U}{\partial X^2} + \frac{\partial^2 U}{\partial Y^2}\right) \tag{2}$$

$$\frac{\partial V}{\partial \tau} + U\frac{\partial V}{\partial X} + V\frac{\partial V}{\partial Y} = -\frac{\partial P}{\partial Y} + Pr\left(\frac{\partial^2 V}{\partial X^2} + \frac{\partial^2 V}{\partial Y^2}\right) + RaPr\theta \tag{3}$$

$$\frac{\partial \theta}{\partial \tau} + U\frac{\partial \theta}{\partial X} + V\frac{\partial \theta}{\partial Y} = \left(\frac{\partial^2 \theta}{\partial X^2} + \frac{\partial^2 \theta}{\partial Y^2}\right) - \frac{\tau^*}{Pl}\left[4\left(\frac{\theta}{T_R} + 1\right)^4 - \int_0^{4\pi} I_R d\Omega\right] \tag{4}$$

$$\frac{\partial \theta}{\partial \tau} = K\left(\frac{\partial^2 \theta}{\partial X^2} + \frac{\partial^2 \theta}{\partial Y^2}\right) + \lambda_i \tag{5}$$

$$\mu\frac{\partial I_R}{\partial X} + \eta\frac{\partial I_R}{\partial Y} + \tau^* I_R = \frac{\tau^*}{4\pi}\left[\omega \int_0^{4\pi} I_R \phi d\Omega' + (1 - \&)I_{Rb}\right] \tag{6}$$

Table 1 summarizes the boundary conditions utilized to solve these equations (Eqs. 1–6).

The non-dimensional parameters and variables that appear in Eqs. 1–6 are:

$$\tau = \frac{\alpha_f t}{H^2}, (U, V) = \frac{(u, v)H}{\alpha_f}, \Delta T = \frac{QH^2}{k_f}, (X, Y) = \frac{(x, y)}{H}, \theta = \frac{(T - T_C)}{\Delta T}, I_R = \frac{i_R}{\sigma T_C^4} \tag{7}$$

$$Pr = \frac{\upsilon}{\alpha_f}, Re = \frac{u_{in}L}{\upsilon}, Ra = \frac{g\beta L^3 \Delta T}{\upsilon \alpha_f}, Pr = \frac{\upsilon}{\alpha_f}, K = \frac{k_s}{k_f}, Pl = \frac{k_f \Delta T}{\sigma T_C^4 H}, T_R = \frac{T_C}{\Delta T} \tag{8}$$

Table 1. Boundary conditions.

Inlet	Outlet	Solid walls
$\theta = 0$ $U = Re \times Pr$ $V = 0$	$\frac{\partial\theta}{\partial Y} = 0$ $\frac{\partial U}{\partial Y} = 0$ $\frac{\partial V}{\partial Y} = -\frac{\partial U}{\partial X}$	$\theta = 0$ at $Y = 1$ $U = V = 0$ $\frac{\partial\theta}{\partial n} = \pm\varepsilon\left(\frac{Q_{Rinc}}{Pl} + I_{Rb}\right)$ at adiabatic walls $\frac{\partial\theta_f}{\partial n} = K\frac{\partial\theta_s}{\partial n} \pm \varepsilon\left(\frac{Q_{Rinc}}{Pl} + I_{Rb}\right)$ and $\theta_f = \theta_s$ at the fluid-cylinder interface

$I_{Rb} = 4\left(\frac{\theta}{T_R} + 1\right)^4$ and ϕ correspond, respectively, to the non-dimensional emission and phase function of the blackbody. (μ, η) are the directional cosines and (ω, τ^*) denote, respectively, the scattering albedo and optical thickness. These latter are set to zero in this study.

The following equation gives the local and mean heat transfer by convection and radiation on the upper wall.

$$Nu_{LC}(X) = -\left.\frac{\partial\theta}{\partial Y}\right|_{Y=1}, \quad Nu_{LR}(X) = \left.\frac{Q_R(X)}{Pl}\right|_{Y=1},$$
$$Nu_{C\ or\ R} = \frac{1}{3-h^*}\int_0^{3-h^*} Nu_{LC\ or\ LR}(X)dX \text{ and } Nu_T = Nu_R + Nu_R \tag{9}$$

2.3 Numerical Approach

The Finite Volume Method (FVM) is employed to discretize the previous equations and boundary conditions. The RTE is integrated using the Discrete Ordinate Method (DOM). A computer program written in FORTRAN is then used to solve the resulting system of equations. The solution is acceptable only if the following condition is satisfied on all variables: $\max\left|\left(\frac{\phi_{i,j}^{new} - \phi_{i,j}^{old}}{\phi_{i,j}^{old}}\right)\right| \leq 10^{-5}$, where ϕ represents a given dependence of the variables (ψ, θ), and i, j are the coordinates of space. A mesh test was done on the accuracy of the results and the computation time, it was found that the mesh 250× 80 gives good results.

To verify its accuracy, the numerical code underwent thorough testing using benchmark problems. The numerical results of Habchi and Acharya [25] in a horizontal channel that include a hot block fixed to the bottom wall were considered. The comparison of velocity obtained before and after the block (Fig. 2) shows a satisfactory matching. More validation of the numerical code with other previous studies can be found in the references [4, 5, 26, 27].

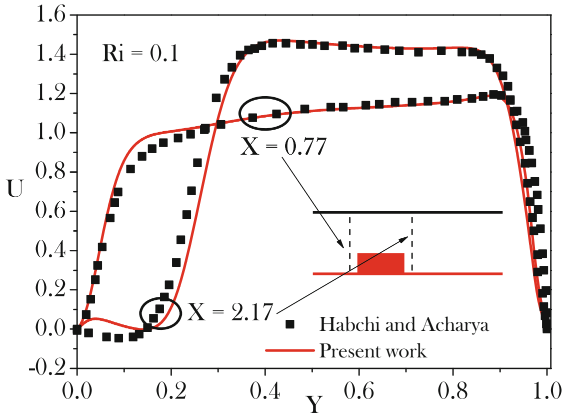

Fig. 2. Comparison of velocity profiles with Habchi and Acharya [25].

3 Results and Discussion

The effect of TR on MC cooling of electronic components simulated by HGBs in a ventilated rectangular channel is demonstrated in this section. The flow structure and thermal field are investigated for various Reynolds number and emissivity. The parameters Ra, D, K, and Pr are set to 2×10^6, 0.4, 0.1, and 0.71, respectively.

The effect of the Reynolds number on the obtained results is analyzed for $\varepsilon = 0$, $h^* = 0.2$. The streamlines (a) and isotherms (b) obtained for various values of Re are shown in Fig. 3. For the case $h^* = 0$, the flow pattern exhibits a bicellular structure. The first cell, (C1), is concentrated around block B1 which generates over 50% of the total heat. The second cell, (C2), surrounds the remaining blocks, but with less intensity. These two cells (C1, C2) rotate in opposite directions, indicating that block B1 establishes the flow direction within the cavity. This behavior can be explained by considering that block B1 generates a considerable amount of heat, creating a thermal plume that induces fluid flow in the cavity. When the mode is changed to MC ($h^* \neq 0$), the cell (C2) is replaced by lines connecting the two openings via different paths. This change in the flow structure can be attributed to the presence of the cooling fluid, which alters the flow pattern and promotes more efficient heat transfer. Figure 3a also demonstrates that when the buoyancy force contribution reduces (Re rises), the number of lines flowing between the cylinders reduces.

According to Fig. 3b, the isotherms are tightly concentrated in the blocks that produce a significant amount of heat ($Q_i > Q$). Conversely, the last two blocks ($Q_i < Q$) appear to be nearly isothermal. The isotherms in the solids show a circular pattern, indicating that the temperature extremes ($\theta_{i,max}$) are located in the center of blocks Bi. This phenomenon can be explained by considering that the heat generated by the blocks is primarily conducted towards the center, where it accumulates, leading to the formation of a hot spot in the middle. At $h^* = 0$, a thermal plume appears over block B1, which generates a significant amount of heat. As the value of Re increases, the influence of buoyancy force decreases, resulting in a gradual reduction in the intensity of the thermal plume. This reduction can be explained by the fact that as Re rises, the inertia of the fluid flow becomes dominant over the buoyancy force, leading to a more streamlined flow pattern.

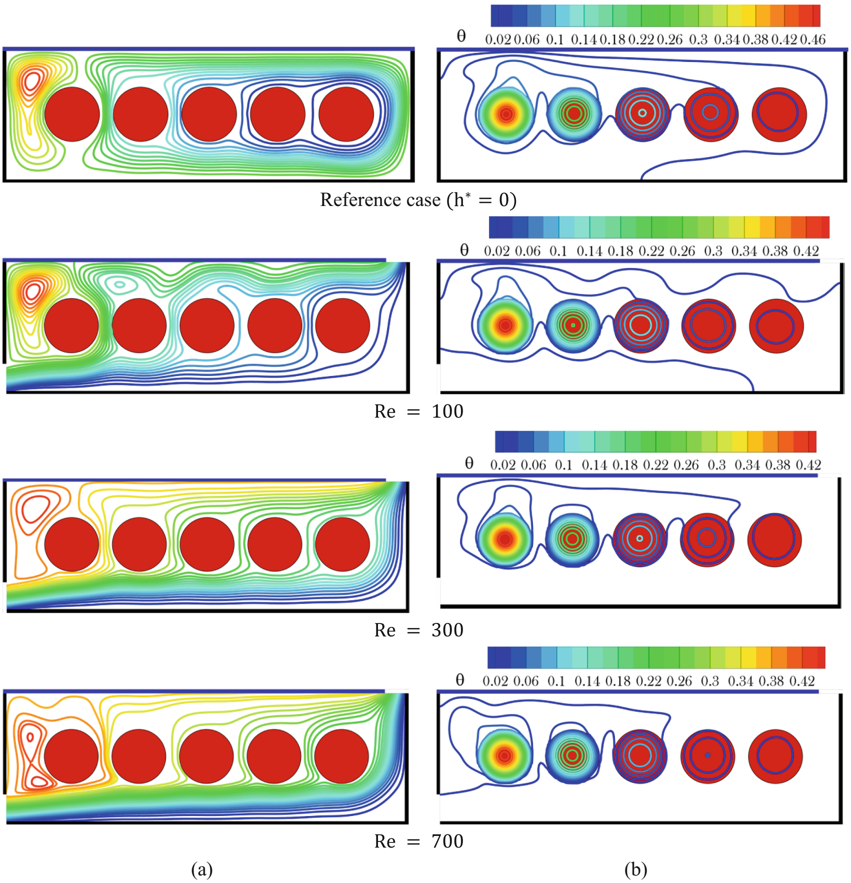

Fig. 3. Streamlines (a) and isotherms (b) obtained for different values of Re with ε = 0.

The profiles of the average convective Nusselt number (Nu_C) and that of the maximum temperature (T_{max}) are plotted in Fig. 4. This figure shows that Nu_C decreases significantly with increasing Re number. For Re = 700, more than 40% of the overall heat generated ($Q_{tot} = 7.75Q$) is removed through the outlet, implying that the cooling method is effective in dissipating a considerable amount of heat from the system. In addition, a decrease of 4.4% is observed in the maximum temperature of block B1. This value reaches its lowest point at Re ≈ 300 before experiencing a slight increase at higher values of Re. These findings suggest that the cooling method (MC) is effective in dissipating heat from multiple components (Bi) that generate varying levels of heat, as long as the Ri number is chosen appropriately (in this case, $Ri = Ra/Re^2Pr \approx 31$).

In other words, the cooling method can effectively dissipate heat in the presence of heat sources if the flow regime is appropriately selected.

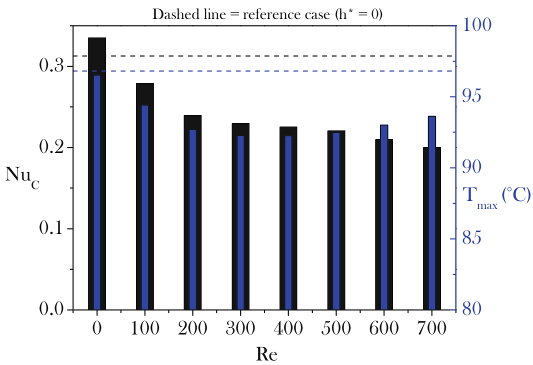

Fig. 4. Maximum temperature and mean convective Nusselt number for various values of Re with $\varepsilon = 0$ and $h^* = 0.2$.

The impact of emissivity on the maximum temperature (T_{max}) and the total heat transfer (Nu_T) within the cavity was studied for $h^* = 0.2(0)$ and Re = 300 (Fig. 5). The results shown in Fig. 5a reveal that T_{max} decreases with ε for both MC ($h^* = 0.2$) and NC ($h^* = 0$) modes. The recorded temperature drop was 3.4% and 5.5% for $h^* = 0.2$ and $h^* = 0$, respectively, indicating the effectiveness of radiative cooling in both modes. This effect can be explained by considering that an increase in emissivity leads to a higher rate of radiation heat transfer, which can dissipate more heat from the system, reducing the maximum temperature. On the other hand, Fig. 5b demonstrates that Nu_T does not exhibit a significant change with an increase in emissivity. For NC mode, the total heat transfer is not dependent on emissivity as all the heat produced is removed by both radiation and convection via the active wall. However, in the MC mode, only a portion of the produced heat is removed through the cold wall, with $Nu_T(h^* = 0.2)/Nu_T(h^* = 0) =$ 71% (78%) for $\varepsilon = 0(1)$.

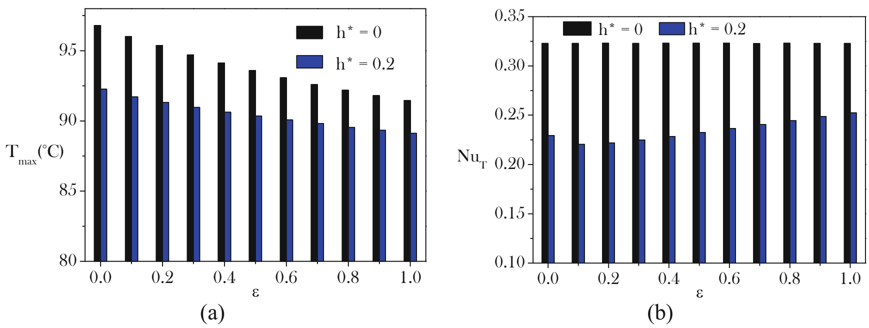

Fig. 5. Maximum temperature (a) and total Nusselt number (b) for Re = 300 and different values of ε.

Overall, these results provide insights into the impact of emissivity on the system's thermal behavior and can be useful for designing cooling systems that incorporate radiative cooling. The results suggest that the effectiveness of radiative cooling can vary depending on the cooling mode and the emissivity of the surfaces.

4 Conclusion

In this paper, coupled thermal radiation and mixed convection in an elongated horizontal ventilated cavity with five heat-generating blocks that generate varying levels of heat have been investigated. The outcomes of the mixed convection mode are contrasted to those found in the case of a closed unventilated cavity (natural convection). The key findings demonstrating the impact of surface emissivity and the Reynolds number are as follows:

- The cavity's maximum temperature decreases by 4.4% as the Re number increases and stabilizes around Re $\approx$ 300.
- An increase in Re reduces lines flowing between the blocks, indicating a decrease in buoyancy contribution.
- The maximum temperature in the cavity reduces by 3.4% and 5.5% for $h^* = 0.2$ and $h^* = 0$, respectively, with an increase in emissivity from 0 to 1, demonstrating the effectiveness of radiative cooling in both mixed and natural convection.

References

1. Pandey, S., Park, Y.G., Ha, M.Y.: An exhaustive review of studies on natural convection in enclosures with and without internal bodies of various shapes. Int. J. Heat Mass Transf. **138**, 762–795 (2019). https://doi.org/10.1016/j.ijheatmasstransfer.2019.04.097
2. Rao, G.M., Narasimham, G.S.V.L.: Laminar conjugate mixed convection in a vertical channel with heat generating components. Int. J. Heat Mass Transf. **50**, 3561–3574 (2007). https://doi.org/10.1016/j.ijheatmasstransfer.2006.12.030
3. Hidki, R., El Moutaouakil, L., Boukendil, M., Charqui, Z., Zrikem, Z., Abdelbaki, A.: Impact of Cu, Al2O3-water hybrid nanofluid on natural convection inside a square cavity with two heat-generating bodies. Mater. Today Proc. **72**, 3749–3756 (2023). https://doi.org/10.1016/j.matpr.2022.09.292
4. Hidki, R., El Moutaouakil, L., Boukendil, M., Charqui, Z., Zrikem, Z., Abdelbaki, A.: Natural convection coupled to surface radiation in an air-filled square cavity containing two heat-generating bodies. Heat Transf. (2022). https://doi.org/10.1002/HTJ.22778
5. Hidki, R., El Moutaouakil, L., Boukendil, M., Charqui, Z., Zrikem, Z.: Mixed-convection coupled with thermal-radiation in a ventilated horizontal channel containing different electronic components. J. Thermophys. Heat Transf. **37**(3), 690–696 (2023). https://doi.org/10.2514/1.T6659
6. Chamkha, A.J., Hussain, S.H., Abd-Amer, Q.R.: Mixed convection heat transfer of air inside a square vented cavity with a heated horizontal square cylinder. Numer. Heat Transf. Part A Appl. **59**, 58–79 (2011). https://doi.org/10.1080/10407782.2011.541216
7. Javadzadegan, A., Joshaghani, M., Moshfegh, A., Akbari, O.A., Afrouzi, H.H., Toghraie, D.: Accurate meso-scale simulation of mixed convective heat transfer in a porous media for a vented square with hot elliptic obstacle: an LBM approach. Phys. A Stat. Mech. its Appl. **537**, 122439 (2020). https://doi.org/10.1016/J.PHYSA.2019.122439

8. Ahammad, M.U., Rahman, M.M., M. L. Rahman: Mixed convection flow and heat transfer behavior inside a vented enclosure in the presence of heat generating obstacle. Int. J. Innov. Appl. Stud. **3**, 967–978 (2013)
9. Ahammad, M.U., Rahman, M.M., Rahman, M.L.: A Study on the governing parameters of mhd mixed convection problem in a ventilated cavity containing a centered square block. Int. J. Sci. Technol. Res. **3**, 273–281 (2014)
10. Rahman, M., Alim, M.A., Saha, S., Chowdhury, M.K.: Mixed convection in a vented square cavity with a heat conducting horizontal solid circular cylinder. J. Nav. Archit. Mar. Eng. **5**, 37–46 (2009). https://doi.org/10.3329/jname.v5i2.2504
11. Rahman, M.M., Billah, M.M., Alim, M.A.: Effect of reynolds and prandtl numbers on mixed convection in an obstructed vented cavity. J. Sci. Res. **3**, 271–281 (2011). https://doi.org/10.3329/jsr.v3i2.4344
12. Gupta, S.K., Chatterjee, D., Mondal, B.: Investigation of mixed convection in a ventilated cavity in the presence of a heat conducting circular cylinder. Numer. Heat Transf. Part A Appl. **67**, 52–74 (2015). https://doi.org/10.1080/10407782.2014.916113
13. Pirouz, M.M., Farhadi, M., Sedighi, K., Nemati, H., Fattahi, E.: Lattice Boltzmann simulation of conjugate heat transfer in a rectangular channel with wall-mounted obstacles. Sci. Iran. **18**, 213–221 (2011). https://doi.org/10.1016/j.scient.2011.03.016
14. Ghaneifar, M., Raisi, A., Ali, H.M., Talebizadehsardari, P.: Mixed convection heat transfer of AL2O3 nanofluid in a horizontal channel subjected with two heat sources. J. Therm. Anal. Calorim. **143**, 2761–2774 (2021). https://doi.org/10.1007/s10973-020-09887-2
15. Hamouche, A., Bessaïh, R.: Mixed convection air cooling of protruding heat sources mounted in a horizontal channel. Int. Commun. Heat Mass Transf. **36**, 841–849 (2009). https://doi.org/10.1016/j.icheatmasstransfer.2009.04.009
16. Boutina, L., Bessaïh, R.: Numerical simulation of mixed convection air-cooling of electronic components mounted in an inclined channel. Appl. Therm. Eng. **31**, 2052–2062 (2011). https://doi.org/10.1016/j.applthermaleng.2011.03.021
17. Hssain, M.A., Mir, R., El Hammami, Y.: Numerical simulation of the cooling of heated electronic blocks in horizontal channel by mixed convection of nanofluids. J. Nanomater. **2020**, 1–11 (2020). https://doi.org/10.1155/2020/4187074
18. Sivaraj, C., Miroshnichenko, I.V., Sheremet, M.A.: Influence of thermal radiation on thermogravitational convection in a tilted chamber having heat-producing solid body. Int. Commun. Heat Mass Transf. **115**, 104611 (2020). https://doi.org/10.1016/j.icheatmasstransfer.2020.104611
19. Saravanan, S., Sivaraj, C.: Combined thermal radiation and natural convection in a cavity containing a discrete heater: effects of nature of heating and heater aspect ratio. Int. J. Heat Fluid Flow **66**, 1339–1351 (2017). https://doi.org/10.1016/j.ijheatfluidflow.2017.05.004
20. Ahmed Mezrhab, M.A., Moussaoui, H.N.: Lattice Boltzmann simulation of surface radiation and natural convection in a square cavity with an inner cylinder. J. Phys. D Appl. Phys. **41**(11), 115502 (2008). https://doi.org/10.1088/0022-3727/41/11/115502
21. Mezrhab, A., Bouali, H., Abid, C.: Modeling of combined radiative and convective heat transfer in an enclosure with a heat-generating conducting body. Int. J. Comput. Methods **02**, 431–450 (2005). https://doi.org/10.1142/S0219876205000521
22. Hidki, R., Moutaouakil, L.E., Boukendil, M., Charqui, Z., Abdelbaki, A.: Natural Convection and Surface Radiation in an Inclined Square Cavity with Two Heat-Generating Blocks. In: Vasant, P., Zelinka, I., Weber, G.-W. (eds.) ICO 2021. LNNS, vol. 371, pp. 948–957. Springer, Cham (2022). https://doi.org/10.1007/978-3-030-93247-3_90
23. Mandal, S.K., Deb, A., Sen, D.: A computational study on mixed convection with surface radiation in a channel in presence of discrete heat sources and vortex generator based on RSM. J. Therm. Anal. Calorim. **141**, 2239–2251 (2020). https://doi.org/10.1007/s10973-020-09774-w

24. Peiravi, M.M., Alinejad, J.: Hybrid conduction, convection and radiation heat transfer simulation in a channel with rectangular cylinder. J. Therm. Anal. Calorim. **140**, 2733–2747 (2020). https://doi.org/10.1007/s10973-019-09010-0
25. Habchi, S., Acharya, S.: Laminar mixed convection in a partially blocked, vertical channel. Int. J. Heat Mass Transf. **29**, 1711–1722 (1986). https://doi.org/10.1016/0017-9310(86)90111-0
26. Hidki, R., El Moutaouakil, L., Boukendil, M., Charqui, Z., Zrikem, Z., Abdelbaki, A.: Mixed convection and surface radiation in a ventilated cavity containing two heat-generating solid bodies. Mater. Today Proc. **66**, 318–324 (2022). https://doi.org/10.1016/j.matpr.2022.05.404
27. El Moutaouakil, L., Boukendil, M., Zrikem, Z., Abdelbaki, A.: Natural convection and radiation in a cavity with a partially heated cylinder. J. Thermophys. Heat Transf. **35**, 312–322 (2021). https://doi.org/10.2514/1.T6097